Influence of temperature on the strength of resistance welded glass fibre reinforced PPS joints

N. Koutras[1], I. Fernandez Villegas[1], R. Benedictus[1]

[1] Aerospace Structures and Materials Department, Delft University of Technology

Abstract

In this work, the effect of temperature exposure on the strength of resistance welded joints is analysed. Glass fibre reinforced polyphenylene sulphide (GF/PPS) adherends were joined using the resistance welding technique, using a stainless steel mesh as the heating element. Single lap shear tests were performed at temperatures ranging between -50 °C and 150 °C to evaluate the strength of the welded joints. The results showed that the lap shear strength decreased with increasing temperature, except for the region between 50 °C and 90 °C where it remained constant. Fractography analysis revealed that the main failure mechanism was glass fibre/matrix debonding and the connection between the mesh and the matrix was not the weakest link at the interface of the joint at any temperatures under study. The fibre/matrix interfacial strength and the stress distribution at the joint overlap were identified as the main factors influencing the behaviour of lap shear strength with temperature.

1. Introduction

Over the last years, high performance thermoplastics, notably polyetheretherketone (PEEK), polyetherketoneketone (PEKK), polyphenylene sulphide (PPS) and polyetherimide (PEI), have gained significant ground in the aerospace industry [1] due to advantageous qualities like their superior damage tolerance, excellent chemical resistance, infinite shelf-life, recyclability, and ability to be welded [2] [3]. Aircraft structures are large and complex and cannot be manufactured in a single step, therefore, joining techniques are utilised in order to connect

different parts together. Hence, joining of polymer composites is of significant importance for the aerospace industry due to the need of reliable, automated and cost-efficient joining methods.

Mechanical fastening is currently the primary joining method used in the aerospace industry, as it possesses several advantages such as process simplicity, through-the-thickness reinforcement and capability for disassembly. In spite of its attractive characteristics, mechanical fastening introduces several problems into a composite structure. In particular, the performance of a joint can be diminished by stress concentrations, delaminations due to hole drilling, additional weight, extensive labour, and coefficient thermal expansion (CTE) mismatch between the composite structure and the fastener [4]. Adhesive bonding minimises stress concentrations, allows for dissimilar materials to be joined and exhibits superior fatigue resistance [5]. However, adhesive bonding has considerable disadvantages as well, such as the need for extensive surface preparation, sensitivity to contamination (e.g. machining oils), limited storage life of uncured adhesives, and long curing times [5]-[7]. Fusion bonding (welding) has been considered as an effective alternative technique for the joining of thermoplastic composites, since it brings several advantages compared to the traditional techniques that can minimise most of these problems. In summary, the principal advantages of welding are the minimised stress concentration, the minimised labour, the very short cycle times and the minimal surface preparation of the substrates [7] [8].

Amongst the various welding techniques, resistance welding is considered as a promising joining technique for thermoplastic composites, which can consistently produce high quality joints with short cycle times, and it has already been successfully used in secondary aircraft structures [1]. Resistance welding is based on Joule heating, which is caused by the circulation of electrical current through a resistive element. Heat dissipation in the resistive element results in polymer melting at the welding interface which allows intimate contact and interdiffusion of polymer chains to take place between the two adherends [7]. The work presented in literature about resistance welding of thermoplastic composites is primarily concerned with the optimisation of the processing parameters, the effect of the heating element and the characterisation of joint strength and failure modes at room temperature. Hou et al. found that the type of the heating element affected the temperature distribution at the weldline as well as

the joint strength [9], while Dubé et al. investigated the influence of the metal mesh geometry; they found that the wire diameter as well as the open gap width had an important effect on the weld quality [10]. Welding time, welding pressure, and power density have been identified as the main factors which govern the welding process and, consequently, the weld quality [11]-[14]. Moreover, the failure modes of resistance welded joints have been classified by several authors, with intralaminar failure being the predominant mode for high quality joints [7] [11] [14].

However, aircraft operate in a wide range of temperatures and can be subjected to extreme conditions. For a transport aircraft, the minimum service temperature is considered -54°C and the maximum temperature, 71°C [15]. However, it is also mentioned that due to operation some components are subjected to temperatures as high as 93°C [15]. Taking this temperature range into consideration, it becomes clear that more knowledge should be gained regarding the exposure of resistance welded thermoplastic composites joints to various temperatures.

In literature, there are extensive studies dealing with the effect of temperature on adhesive joints. The strength of adhesively bonded fibre reinforced polymer double lap joints has been reported to decrease with increasing temperature, while the failure mode at high temperatures changed from adherend failure to adhesive failure [16] [17]. Adams et al. studied the exposure of adhesive single lap joints to a wide range of temperatures (-60°C, 200°C) and found that the joint strength decreased at low and high temperatures because the adhesive became brittle and soft respectively [18]. Da Silva and Adams studied the effect of temperature on titanium/composite double lap joints and found that the failure of the joints at -55°C and 22°C occurred through the thickness of the composite [19]. The same authors investigated the mixed modulus concept of low temperature and high temperature adhesives and suggested that for dissimilar adherend double lap joints, the use of a high modulus adhesive and a low modulus adhesive improved the performance compared to the high modulus adhesive alone [20].

Although as briefly outlined before much research is described in literature about the influence of temperature on bonded joints in fibre reinforced polymers, to the authors' knowledge there are no studies currently available on the influence of temperature on resistance welded polymer composite joints. Despite obvious similarities between bonded joints and welded joints (i.e. joint architecture, continuous joint nature, polymer-rich joint interface), they hold several fundamental

differences which may cause different temperature-dependent mechanical performances. These fundamental differences concern the joining mechanisms, i.e. adhesive forces versus molecular inter-diffusion, and the architecture and nature of the joint interface, i.e. dissimilar polymer versus matrix polymer with embedded metal mesh. Likewise, available knowledge on the effect of temperature on the behaviour of fibre reinforced composites is not directly applicable to resistance welded joints owing to the complexity of the weld interface. In particular, the effect of varying temperature could be detrimental to the strength of the welded joints by virtue of the nature of the bond between the metal mesh and the polymer matrix at the weld interface. Resistance welded joints feature a rather complex resin-rich welding interface with an embedded resistive heating element, generally a metal mesh. It is known that the mechanism dictating the bond between metals and polymers is mechanical interlocking [5] [21]. During the welding process, the polymer matrix wets and penetrates the irregularities of the metal surface and the mesh open gaps, locking itself mechanically to the metal wires. This mechanism is promoted by the residual thermal stresses that are formed during the cooling process. As the thermoplastic cools down from its melt, it shrinks and contracts more than the metal due to their CTE mismatch, thereby, resulting in compressive stresses on the metal wire. Consequently, at room temperature the polymer matrix and the metal mesh form a strong connection, as was demonstrated in a previous study where the main failure at room temperature, in GF/PEI and GF/PPS resistance welded joints, was found to be glass fibre/matrix debonding [11]. However, when the joints are subjected to higher temperatures, the opposite effect will occur. In particular, at high temperatures the compressive stresses will be lowered due to the higher thermal expansion of the polymer over the metal wires, resulting in a diminished mechanical interlocking, which could have a detrimental effect on the joint strength. Therefore, even if the stainless steel mesh does not have a negative impact on the mechanical performance of resistance welded joints at room temperature conditions, it could still be the primary reason for joint failure at high temperatures.

Hence, two key questions arise which require further investigation in order to develop a comprehensive understanding of the behaviour of resistance welded thermoplastic composite joints at different temperatures.

- Is the connection between the metal mesh and the thermoplastic matrix the weakest link at the welding interface when the joints are subjected to elevated temperatures?
- How is the weld strength affected by temperature?

To fill this gap, this paper analyses the strength and failure mechanisms of resistance welded glass fibre reinforced PPS joints tested at a wide range of temperatures using a fully experimental approach. The major objective of this study is to evaluate in detail the relationships between the joint strength and the constituents of the joint, namely the fibres, the thermoplastic matrix and the metal mesh, under the influence of temperature.

2. Experimental Procedure

2.1 Laminate Manufacturing

The material used in this study was Cetex® woven (eight harness satin) glass fibre reinforced polyphenylene sulphide composite (GF/PPS) supplied by Ten Cate Advanced Composites, The Netherlands. Laminates measuring 580 mm x 580 mm were built from semi-impregnated GF/PPS layers with a stacking sequence of [(0°/90°)4]s. The laminates were consolidated using a hot platen press at 320°C and 1 MPa pressure for 20 min. The cooling rate of the press plates was consistently set at 15°C/min for all the laminates manufactured in this study. The stainless steel moulds used in the press consolidation process were first cleaned with acetone, then degreased with PFQD degreasing agent (Socomore) and finally coated with Marbocote 227CEE release agent. The final thickness of the consolidated laminates was 1.9 mm. Welding adherends and test specimens were cut from the consolidated laminates using a water-cooled diamond blade.

2.2 Resistance Welding

The in-house developed resistance welding setup shown in Figure 1 was used in this work. The main elements in this setup are: (a) DC power supply unit with a maximum power output of 45A/70V (Delta Electronika, The Netherlands), (b) pneumatic cylinder to provide both the welding pressure and the clamping pressure, (c) copper connectors, (d) thermal insulation blocks made out of ceramic blocks, (e) computer equipped with dedicated LabView software for welding process control, (f) data acquisition system (DAQ). A plain woven stainless steel (AISI 304L) mesh with 0.04 mm wire diameter and 0.09 mm open gap width (Dinxperlo, The Netherlands) was used as the heating element in the welding process based on the results presented in [10]. The dimensions of the heating element were 300 mm x 13 mm. A 90 µm-thick neat amorphous PPS film (Amcor Flexibles, Gent, Belgium) was placed between the metal mesh and the top adherend for adequate filling of the open areas in the mesh during the welding process. The adherends, with dimensions 102 mm x 171 mm, were welded in a single lap configuration with overlap dimensions 171 mm x 13 mm. Both adherends and the heating element were degreased (PFQD degreasing agent) prior to welding. The welding parameters, resulting from an optimization performed in a previous study [22], were 80 kW/m2 power density, 0.8 MPa welding pressure and 55 s heating time.

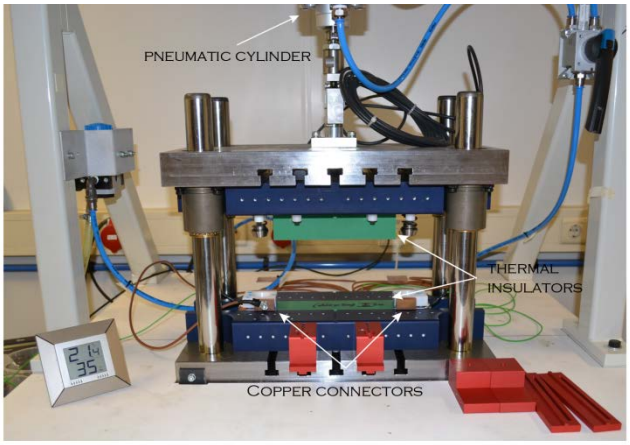

Figure 1. Resistance Welding set-up. The different parts of the device are indicated on the figure.

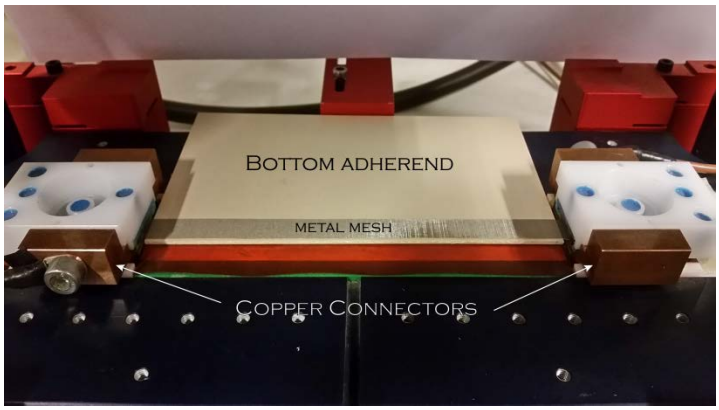

Figure 2. Preparation of resistance welded joints. The metal mesh is placed over the bottom adherend while being in good contact with the copper connectors in order to ensure electrical current circulation.

2.3 Material Characterisation

2.3.1 Physical Analysis

Dynamic Mechanical Analysis (DMA) was used to measure the glass transition temperature and the evolution of the storage and loss moduli of the PPS resin and the GF/PPS composite. Three point bending DMA tests were carried out in a Pyris Diamond DMA from Perkin Elmer, from -70°C to 200°C, at a frequency of 1Hz and a heating rate of 2°C/min. The dimensions of the specimens were 40 mm x 15 mm x 2 mm for the neat PPS and 40 mm x 13 mm x 1.9 mm for the GF/PPS composite.

Thermomechanical Analysis (TMA) was used to measure the CTE of PPS within -70°C to 200°C temperature range. The TMA experiments were carried out on a 15 mm x 3 mm x 90 µm PPS film sample supplied by Amcor Flexibles (Gent, Belgium) at a heating rate of 2°C/min in a Diamond TMA from Perkin Elmer.

Liquid nitrogen was used in both the DMA and TMA tests in order to reach the cryogenic temperatures.

2.3.2 In-plane Shear Tests

For the determination of in-plane shear (IPS) strength and modulus at different temperatures within the -50°C to 120°C range, ±45° tensile tests were performed in a Zwick 250kN machine, according to the ASTM D3518 standard [23]. The relative deviation of the machine was ±0.65% in the range of 500N, and below ±0.04% for higher loads. The ±45° tensile test was chosen as an evaluation method because it is a simple test in terms of fixture and specimen preparation and it has been proven to be sensitive to the interfacial shear strength [24]. This was motivated by the findings by Shi et al. who identified fibre/matrix debonding as the main failure mechanism of resistance welded GF/PPS and GF/PEI joints tested at room temperature [22]. The test specimens were cut in the ±45° direction of the fibres, using a water cooled diamond blade. The specimens were 250 mm-long, 25 mm-wide and 1.9 mm-thick. 50 mm-long paper tabs were bonded on the specimens using a cyanoacrylate adhesive (RS Components) in order to prevent slippage during testing. 0°/90° biaxial rosette strain gauges from Kyowa (KFG-5-120-D16-23) with 5 mm gauge length were bonded to the middle section of the specimens (Cement Glue CC-33A, Kyowa) for in plane strain measurements (parallel and transverse to the longitudinal direction of the samples). The temperature chamber used for the tests was pre-heated for 1 hour at the test temperature and the specimens were pre-conditioned for 30 minutes prior to the tests. Liquid nitrogen was used for the tests at -50°C. All tests were conducted in displacement control at a loading rate of 2 mm/min.

In total three specimens per temperature were tested and used to calculate the average shear stress and the average shear modulus. It must be noted that, following the guidelines in the ASTM D3518 standard, the in-plane shear strength was calculated at 5% shear strain, since at this strain level the fibre rotation is small and hence the difference between apparent and actual shear stresses can be expected to be small, as reported by Wisnom [25]. The in plane shear modulus was calculated in the initial elastic region, i.e. in the 0.01 % – 0.1 % strain range.

The in-plane shear strain, γ_{12}, was calculated as:

$$\boldsymbol{\gamma_{12} = \varepsilon_{yy} - \varepsilon_{xx}} \quad \textbf{(1)}$$

where ε_{yy} is the longitudinal strain and ε_{xx} is the transverse strain.

The in-plane shear stress, τ_{12}, was calculated as:

$$\tau_{12} = \frac{F}{2*w*t} \quad \textbf{(2)}$$

where F is the applied load in [N], and w and t, the width and thickness in [mm] respectively.

2.4 Characterisation of Welded Joints

2.4.1. Lap Shear Tests

From each welded sample, five single lap shear specimens were cut using a water-cooled diamond blade with a final width of 25.4 mm. Single lap shear tests based on the ASTM D 1002 standard [26] were performed at different temperatures within the -50°C to 150°C range. A 250kN Zwick/Roell universal testing machine with less than ±0.04% deviation at all loads except for a ±0.65% deviation around 500N, operating at 1.3 mm/min cross-head speed, and a temperature chamber were used for the tests. The temperature chamber was pre-heated for 1 hour at the test temperature and all specimens were maintained at the test temperature for 30 minutes prior to testing in order to reach equilibrium of the entire specimen. Liquid nitrogen was used to perform the tests at -50°C. The apparent lap shear strength (LSS) of the resistance welded joints was calculated as the maximum load divided by the overlap area (25.4 mm x 13 mm). The total number of specimens tested at each temperature is shown in Table 1**.**

Table 1. Number of single lap joint specimens tested at each temperature.

Test Temperature (±2°C)	**-50**	**20**	**50**	**70**	**90**	**120**	**150**
# of specimens	9	43	16	15	15	10	8

2.5.1 Fractography

Fractography was used to investigate the failure mechanisms of the welded joints. For this purpose a stereo microscope (Zeiss stereo Discovery V8) and a scanning electron microscope (JEOL JSM-7500F) were used. Image J (open source software) was used to calculate the size of areas of interest on the fracture surfaces.

3. Results

3.1 Material Characterisation

3.1.1 Physical Analysis

The thermal evolution of the loss and the storage moduli of the PPS resin and the GF/PPS composite, as resulting from DMA tests, is shown in **Figure 3**. The loss modulus of both the neat PPS resin and the GF/PPS composite exhibited a peak with a maximum at around 103°C, which defines the Tg of the polymer and, as expected, it coincided with a significant drop in the storage modulus. In the case of the GF/PPS composite a secondary smaller peak with onset at around 50°C was also observed in the loss modulus. At that temperature the storage modulus of the composite was found to already start slowly dropping. It is worth mentioning that both the storage and the loss modulus of the GF/PPS composite showed a slight sudden increase towards the end of the DMA test (i.e. at around 200°C). Possible reasons for this peculiar behaviour could be either a test artefact or interaction between the reinforcing fibres and the loading nose, although further tests would be necessary to clarify it. Such research is however out of the scope of this paper, where the temperature range of interest was between -50 and 150°C.

Table 2 shows the linear CTE values of all materials in the adherends (matrix and reinforcing fibres) and in the weld line (matrix and metal mesh). It should be noted that the CTE of thermoplastic resins exhibits a discontinuous jump in the glass transition region owing to increased chain mobility which precludes proper measurements in that region. The plot in Figure 4, which depicts the dimensional changes of an originally amorphous PPS film during TMA analysis, shows indeed a sudden increase in slope at 83°C, related to glass transition, as well as an exothermic signal at 110°C, potentially due to cold crystallization. Owing to this behaviour, it was quite difficult to obtain accurate CTE values at 90°C and 120°C and hence, only the CTE values for the ranges (-30°C, 70°C) and (135°C, 200°C) are reported in this work.

The CTE values below -30°C are not included in the table because of the relatively large noise level at cryogenic temperatures. However, it could be assumed that the CTE values at -50°C do not vary much compared to the values at -30°C owing to the very limited mobility of the polymeric chains at very low temperatures.

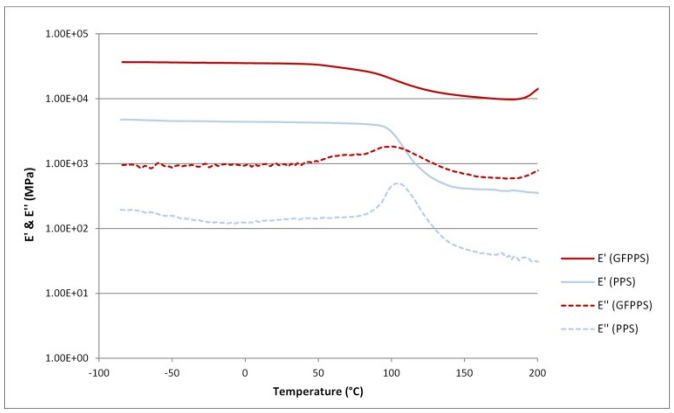

Figure 3. Storage modulus (E') and loss modulus (E'') as a function of temperature for GF/PPS and neat PPS.

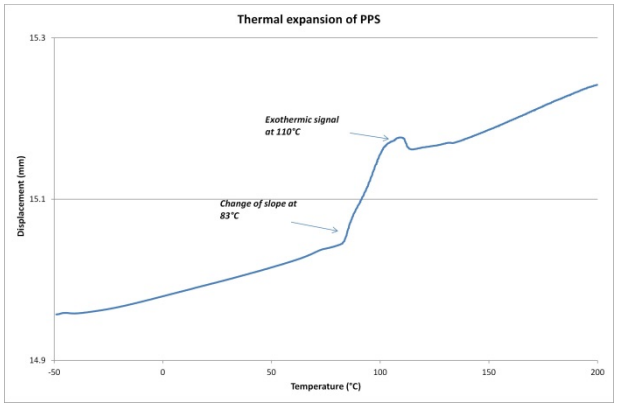

Figure 4. Thermal expansion of PPS as resulting from TMA tests (2°C/min)

Table 2. Linear CTE values for materials in adherends and weld line.

Material	**CTE (10^{-6} /°C)**	**Comments**
PPS	48.0 (-30°C to 70°C) 74.0 (135°C to 200°C)	Obtained through TMA tests
Stainless Steel 304L	17.8 (10°C to 315°C)	Obtained from [27]
Glass Fibres	5.0 (-)	Obtained from [28]

3.1.2 In-Plane Shear Tests

Figure 5 shows that the temperature increase had a detrimental effect in both the in-plane shear strength and the in-plane shear modulus. As seen in **Figure 5**, both the strength and modulus seemed to have a more pronounced decrease rate in the 50°C to 90°C range. It should be noted that in the tests at 120°C the adhesive used to glue the strain gauges on the specimens failed at around 2% shear strain, therefore it was not possible to measure the IPS strength but only the modulus.

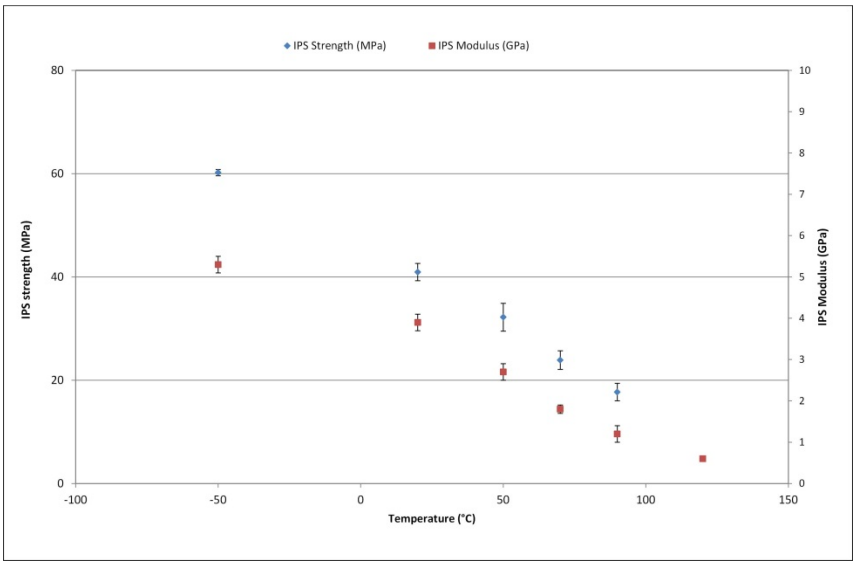

Figure 5. Effect of temperature on IPS properties of GF/PPS laminates. The corresponding average values of IPS strength were calculated at 5% shear strain while the IPS modulus was calculated in the initial elastic region (0.01% - 0.1%). The scatter bars represent the standard deviation.

3.2 Characterisation of Welded Joints

3.2.1 Lap Shear Strength

Figure 6 and **Table 3** show the average values and corresponding scatter for the apparent lap shear strength (LSS) of the welded joints as a function of testing temperature. As it can be

seen, the LSS showed an overall decreasing trend with increasing temperature, except for the region between 50°C and 90°C where the LSS exhibited a plateau. Therefore, the plot in **Figure 6** could be divided into three distinct regions according to the temperature dependence of the LSS. Region A extended from -50°C to 50°C and featured an approximately linear decrease of LSS with increasing temperature. As it is, the LSS was found to increase in 28% between room temperature (RT) and -50°C. Likewise, increasing the temperature from RT to 50°C caused a 12% LSS decrease. Region B extended from 50°C to 90°C and, as previously mentioned, was characterised by a LSS plateau. Finally, region C, which extended from 90°C to 150°C, featured an approximately linear drop in LSS. Relative to RT, a 25% and 35% LSS decrease was measured at 120°C and 150°C, respectively.

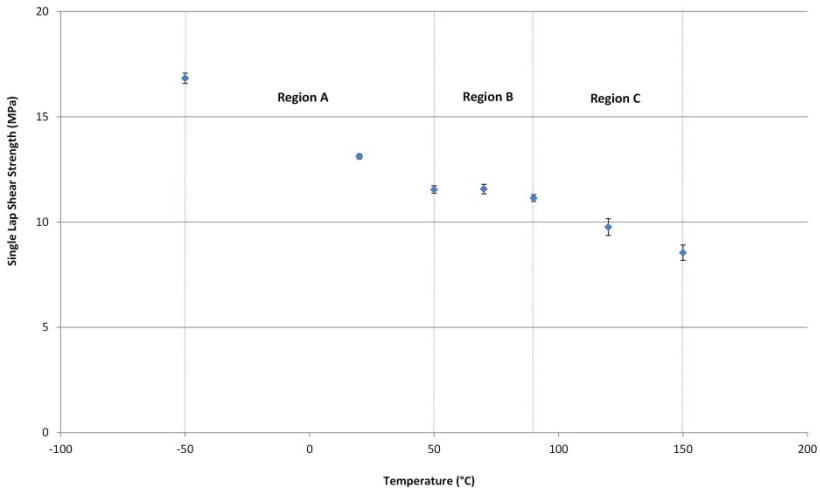

Figure 6. Influence of temperature on the single lap shear strength of resistance welded GF/PPS joints. Scatter bars represent standard deviation values.

Table 3. Summary of single lap shear test results on GF/PPS laminates at [-50°C, 150°C].

Temperature	**LSS (MPa)**
-50°C	*16.8 ± 0.4*
20°C	*13.1 ± 0.4*
50°C	*11.5 ± 0.4*
70°C	*11.6 ± 0.5*
90°C	*11.1 ± 0.3*

120°C	*9.8 ± 0.6*
150 °C	*8.5 ± 0.7*

3.2.2 Fractography

In order to understand the effect of temperature on the failure mechanisms of the resistance welded GF/PPS joints, the fracture surfaces of the tested specimens were investigated. Fractographic analysis was carried out at two levels: naked-eye observation to investigate macroscopic failure features and scanning electron microscopy to investigate microscopic failure features.

Macroscopic failure features

The fracture surfaces of welded joints tested at -50°C and RT (an example of which is shown is **Figure 7**) showed that approximately 50% of the metal mesh, mostly covered by resin and glass fibres, remained on each side of the fracture surface. Owing to the peel stress concentrations at the edges of the overlap in single lap shear joints [29] (**Figure 8)** and to the resin and fibres covering the fractured mesh, failure was believed to initiate in both adherends and to progress towards the middle of the joint overlap where mesh tear eventually occurred, as shown in the schematic in Figure 9 . As a result of this type of failure, hereafter referred to as fracture type I, roughly the same area of mesh (between 40% and 60% of the total mesh area) was left on each mating fracture surface (**Figure 9**). The fracture surfaces of resistance welded joints tested at T ≥ 50°C revealed some changes in how the mesh was divided between the two mating fracture surfaces after failure. **Figure 10** illustrates the top fracture surfaces of welded joints tested at 70°C, 90°C and 120°C where these changes can be observed. Consequently, two additional fracture types were defined, fracture type II (60%-80% of the mesh on one of the fracture surfaces) and fracture type III (80%-100% of the mesh on one of the fracture surfaces), as

shown in the schematic representations in **Figure 11**. **Figure 12** shows the percentage of specimens that exhibited the three fracture types defined above per test temperature as well as the LSS per group of specimens (defined by fracture type and testing temperature). It can be seen that, apart from the fact that specimens tested at -50°C and RT exclusively showed fracture type I, at 50°C and 70°C fracture type I was prevalent, at 90°C the dominant fracture type was type III, while at 120°C and 150°C the distribution of the fracture types was more uniform. Nevertheless, there was no clear trend on a prevalent fracture type at temperatures above RT. The macroscopic failure was found to be independent of the position of the adherends during the resistance welding process. Similarly, the clamping position of the adherends during the single lap shear tests had no contribution to the change in macroscopic failure. It should be noted that, as seen in **Figure 12**, the macroscopic fracture type did not seem to have any significant effect on the LSS of the welded joints.

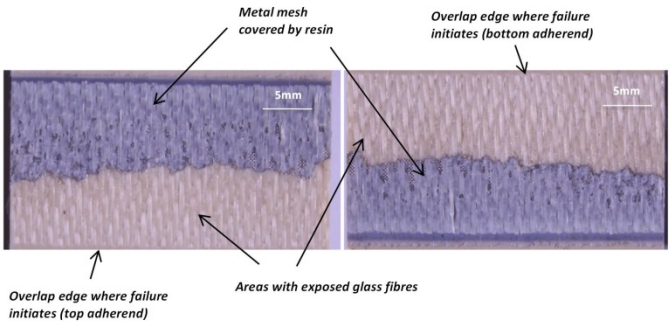

Figure 7. Mating fracture surfaces of a specimen tested at -50°C. The arrows indicate the areas where the metal mesh is mostly covered by PPS resin as well as the areas with exposed glass fibres, In addition, the overlap edges where failure was initiated are also indicated.

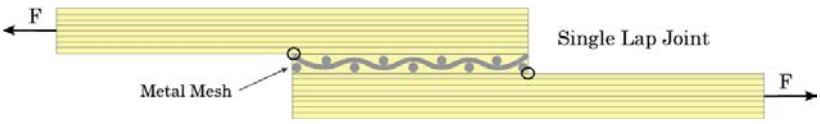

Figure 8. Schematic of a resistance welded single lap shear sample with circles indicating the locations of peel stress concentrations.

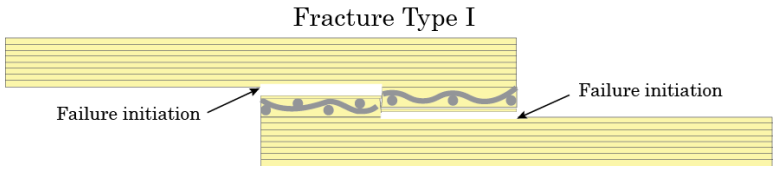

Figure 9. Schematic of failure observed in samples tested at -50°C and room temperature: Fracture Type I (40-60% of metal mesh on one side).

Figure 10. Representative fracture surfaces of welded joints tested at 70°C (left) showing fracture type II, 90°C (middle) and 120°C (right) showing fracture type III Only one fracture surface is provided per testing temperature.

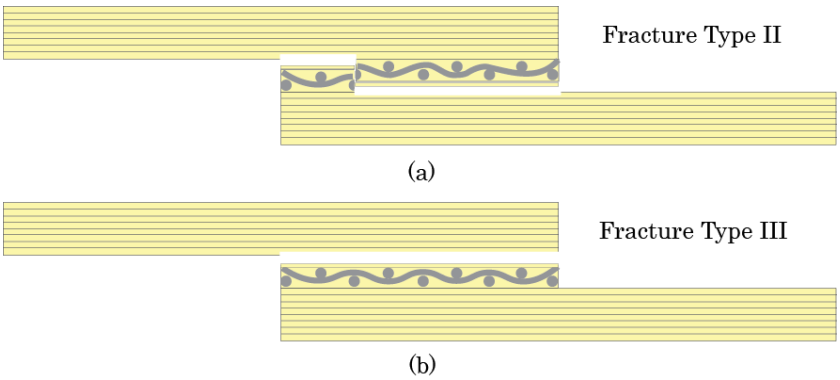

Figure 11. Schematic representation of failure (a) fracture type II (60-80% of metal mesh on one side) and (b) fracture type III (80-100% of metal mesh on one side).

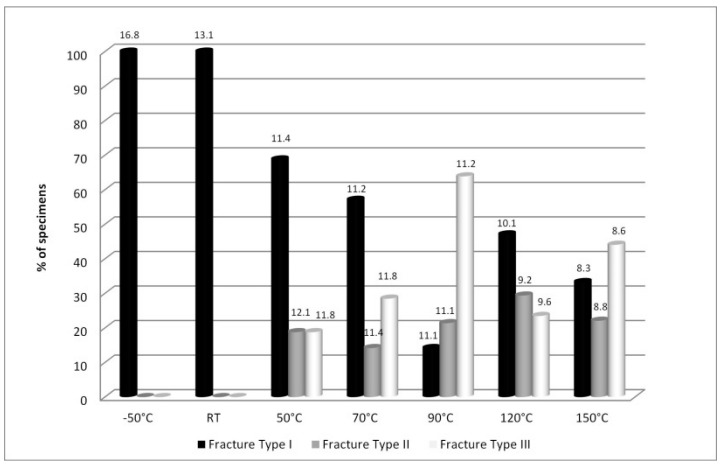

Figure 12. Distribution of fracture types as a function of temperature. The LSS values corresponding to each group of samples (defined by fracture type and testing temperature) are shown on top of the bars.

Microscopic failure features

All tested specimens exhibited the same key microscopic failure mechanisms regardless of the test temperature. These key mechanisms were fibre/matrix debonding and mesh/matrix debonding. Among these, fibre/matrix debonding was found to be the predominant failure mechanism at all temperatures. This is illustrated by the fracture surfaces in **Figure 13** and **Figure 14**, corresponding to a specimen tested at -50°C and a specimen tested at 120°C, respectively. Finally, the cross-section micrograph of a single lap shear specimen tested at RT shows that fibre/matrix debonding not only did occur at the weld line but also within the bulk of the composite in the overlap (**Figure 15**).

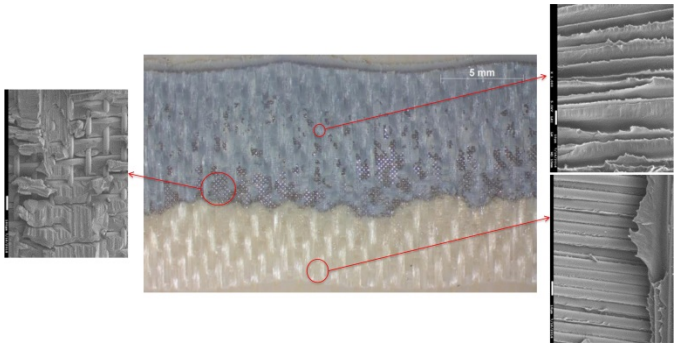

Figure 13. Fracture surface of specimen tested at -50°C (centre). SEM micrographs illustrate fibre/matrix debonding (right) and mesh/matrix debonding (left). The top right SEM image illustrates fibre imprints in the resin and the bottom right SEM image illustrates debonded fibres.

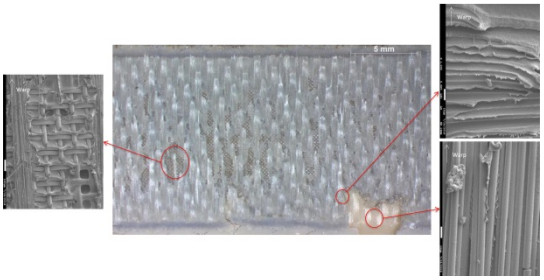

Figure 14. Fracture surface of specimen tested at 120°C (centre). SEM micrographs illustrate the fibre/matrix debonding (right) and mesh/matrix debonding (left). The top right SEM image illustrates fibre imprints in the resin and the bottom right SEM image illustrates debonded fibres.

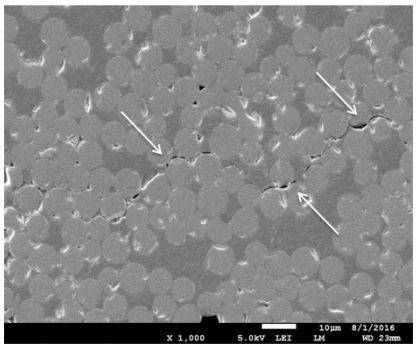

Figure 15. SEM image of a cross-section of specimen tested at RT showing fibre/matrix debonding. The arrows indicate the failure which occurs within the weft bundle and along the fibre/matrix interface.

4. Discussion

In this section the results are discussed from the perspective of the key research questions that motivated the present research, i.e. (a) is the connection between the metal mesh and the thermoplastic matrix the weakest link at the welding interface when the joints are subjected to elevated temperatures and (b) how is the joint strength affected by the temperature?

Regarding the first question, even though the PPS matrix was found to expand significantly more than the metal mesh (2.5 and 4 times more, below and above its Tg, respectively), the resulting decrease in the compressive stresses on the mesh was not enough to turn the mesh/matrix connection into the weakest link in the welded joints at least up to 150°C. This statement is supported by the fact that fibre/matrix debonding, and not mesh/matrix debonding, was found to be the primary microscopic failure mode not only at low but also at elevated testing temperatures. The relatively big differences between the melt crystallization temperature of PPS and the test temperatures are believed to favour this behaviour. Likewise, the fact that during lap shear testing the highest stresses occur at the interface between the adherend and the weld line [29] and not at the centre of the weld line, i.e. the location of the mesh, could as well play a role.

Regarding the second question, the strength of the welded joints showed an overall decreasing trend with increasing temperature with the exception of the 50°C to 90°C range, where the weld

strength remained fairly constant. The test temperature was found to affect to some extent the macroscopic failure type, however there seemed to be no apparent link between the macroscopic failure type and the weld strength. Microscopic failure features pointed at fibre/matrix interfacial strength as the main responsible for the strength of the welded joints at all test temperatures. Consequently, fibre/matrix interfacial strength was identified as one of the potential main factors affecting the thermal evolution of the weld strength. Moreover, given the sensitivity of lap shear tests to the mechanical properties of adherends and weld line [30], the stress state at the overlap was identified as another potential influential factor. It follows a more detailed discussion on the effect of temperature on these two factors.

In thermoplastic composites fibre/matrix interfacial strength is often related to the residual thermal stresses caused during manufacturing as well as the static friction at the fibre/matrix interface which result in mechanical interlocking between the matrix and the fibres [31][32]. Residual thermal stresses, more specifically residual compressive stresses on the surface of the fibres, originate from the CTE mismatch between fibres and matrix, similarly to the mesh/matrix case discussed before. Consequently, the residual compressive stresses are directly proportional to the elastic modulus of the matrix, the CTE difference between matrix and fibres and the difference between the melt crystallization temperature of the matrix, i.e. stress-free temperature, and the service temperature [31][33]. An increase in the testing temperature hence tends to decrease the residual compressive stress on the fibres through a decrease in the temperature gap between stress-free and service temperatures. However, based on the analysis of the storage modulus of PPS (see **Figure 3**), the biggest decrease in the compressive stresses is caused by the fact that the elastic modulus of the matrix is one order of magnitude lower above the glass transition temperature. The increase of the CTE difference between fibres and matrix above the Tg of PPS (see **Table 2**) is, on the contrary, too small to counteract the effect of the drop in elastic modulus. The results of the in-plane shear tests (see **Figure 5**) did show a decrease in IPS strength, which according to [24] can be related to a decrease in the fibre/matrix interfacial strength, with increasing temperature. Interestingly the IPS strength decreased at a faster pace in the 50°C to 90°C temperature range, which does not seem to be related to the above-mentioned changes in the residual compressive stresses on the fibres. It might however result from potential temperature-induced changes in the sizing of

the glass fibres which could affect its interaction with either the matrix or fibres themselves. The premature decrease in storage modulus and secondary peak in the loss modulus observed in the same temperature range for the GF/PPS composite (see **Figure 3**) are in line with this hypothesis since they seem to indicate the presence of sizing on the glass fibres with a lower Tg than the PPS matrix [32] [33]. Further research is however needed to fully understand this behaviour. It is also worth noticing that the IPS modulus followed the same trend as the IPS strength. The fact that the storage modulus of PPS remains virtually constant from -50°C till 90°C suggests that the decrease in IPS modulus could as well be linked to the decrease in fibre/matrix interfacial strength. This hypothesis is in line with the findings of some researchers [32][35], however there is no consensus in literature regarding the presence or absence of a relationship between the fibre/matrix interfacial strength and the in plane shear modulus [24].

With regards to the stress state in the joint overlap during single lap shear testing, it is well known that the geometry of a single lap joint results in non-uniform stress distributions with shear and peel stress concentrations at the edges of the overlap [20][36]. Of these, the peel stresses are the most critical ones in composite welded joints [37]. The magnitude of the shear and peel stress peaks is dependent, among other factors, on the deformations in the adherends and on the deformation in the adhesive, i.e. the weld line. In particular, secondary bending of the adherends, which results from the eccentric load path inherent to the sample geometry, is known to increase the peel stresses at the edges of the overlap [36] [38]. Likewise, the longitudinal deformation of the adherends and of the adhesive affect how uniform the shear stress distribution is at the overlap. Increasing the stiffness of the adherends and/or decreasing the stiffness of the adhesives results in more uniform and hence more favourable shear stress distributions at the overlap [30]. Finally, the shear deformation of the adherends causes the stresses to be distributed over a larger area hence decreasing the shear stress concentrations [39]. Consequently, by affecting the stiffness of the adherends and of the weld line, the testing temperature has an effect on the distribution of the shear stresses along the overlap and the magnitude of the peel stress peaks at the edges of the overlap. Particularly, in the -50°C to 50°C testing temperature range the decrease in IPS modulus of the adherends with increasing temperature can be expected to have a positive effect in the load distribution within the overlap by decreasing the shear stress concentrations at the overlap edges. Between 50°C and 90°C,

the decrease in IPS modulus and hence its positive effect in the shear stress distribution is more pronounced. Above 90°C the positive effect brought along by the decrease in IPS modulus is counteracted by the increase in peel stresses resulting from a significant decrease in the storage modulus of the adherends.

Consequently, in the whole temperature range considered in this study (i.e. -50°C to 150°C) the fibre/matrix interfacial strength decreased with increased temperature. Given the fact that fibre/matrix debonding was found to be the major failure mechanism of the welded joints, the stress values resulting in failure of the welded joints decreased with increased temperature. This would have resulted in a continuous decrease of the lap shear strength of the welded joints with increasing temperatures if the stress distribution within the overlap had been the same for all testing temperatures. However, the sensitivity of the lap shear test to the stiffness of the welded coupons resulted in a dependence between the stress distribution at the overlap and the testing temperature which affected lap shear strength results. Particularly, the pronounced decrease in IPS modulus between 50°C and 90°C most likely counteracted the decrease in failure strength by decreasing the shear stress concentrations and hence caused the observed discontinuity in the lap shear strength of the welded joints.

5. Conclusions

The major objective of this study was to evaluate in detail the relationships between the joint strength and the constituents of the joint, namely the glass fibres, the PPS matrix and the stainless steel mesh, under the influence of temperature. Single lap shear tests were performed at temperatures ranging between -50°C and 150°C to assess the strength of the welded joints, followed by a detailed fractography analysis which identified the main failure mechanisms. The following conclusions can be drawn:

- The strength of the resistance welded joints showed an overall decreasing trend with increasing temperature, except for the region between 50°C and 90°C, where the weld

strength remained fairly constant. At -50°C the LSS was 28% higher than the strength at room temperature while the lowest strength was observed at 150°C, exhibiting a 35% decrease with respect to room temperature.

- Fractographic inspection revealed that the main failure mechanism of resistance welded GF/PPS joints at all temperatures was fibre/matrix debonding. This type of failure could be favoured by the relatively big differences between the melt crystallisation temperature of PPS and the test temperatures, and by the high stresses at the interface between the adherend and the weldline instead of the centre of the weldline, where the mesh is located. Hence, the connection between the stainless steel mesh and the PPS matrix was not the weakest link at the interface of the single lap joint at any of the temperatures under study.

- The decrease in IPS strength with increasing temperature together with the fact that fibre/matrix debonding was found to be the main failure mechanism at all temperatures, suggested that the fibre/matrix interfacial strength was the main factor affecting the strength of the resistance welded joints. This reduction in fibre/matrix interfacial strength was mainly attributed to the decrease in the residual compressive stresses between the glass fibres and the PPS matrix, which was even more pronounced at temperatures above Tg due to the significant drop of the PPS modulus at these temperatures.

- The stress state at the overlap was identified as a potential influential factor for the discontinuity in the lap shear strength in the temperature region between 50°C and 90°C. The pronounced decrease in IPS modulus could cause the stresses to be distributed over a larger area, thus, lower the shear stress concentrations which potentially could counteract the decrease in the failure strength of the welded joints caused by the decrease in fibre/matrix interfacial strength.

Acknowledgements

This study is part of the Thermoplastic Affordable Primary Aircraft Structure 2 (TAPAS2) project, financed by Netherlands Enterprise Agency of the Ministry of Economic Affairs. The authors would also like to thank Dr. Roger Groves, Dr. Calvin Rans, Dr. Dimitrios Zarouchas, and Dr. John-Alan Pascoe, for the many valuable discussions, and Martino Marchetti for the technical support in the thermal analysis experiments.

References

[1] Offringa A. New thermoplastic composite design concepts and their automated manufacture. JEC Composites Magazine 2010; 58 (June-July): 45-49.

[2] Ibeh CC. Thermoplastic Materials: Properties, Manufacturing Methods, and Applications. Boca Raton, FL: CRC Press, Taylor & Francis Group, 2011.

[3] Jones DP, Leach DC, Moore DR. Mechanical properties of poly(ether-ether-ketone) for engineering applications. Polymer 1985; 26(9): 1385-1393.

[4] Campbell FC. Structural Composite Materials. Ohio: ASM International, 2010.

[5] Pocius AV. Adhesion and Adhesives Technology. Munich: Hanser 3rd edition, 2012.

[6] Niu MCY, Composite Airframe Structures, Practical Design Information and Data. Hong Kong: Conmilit Press Ltd, 1st edition, 1992.

[7] Ageorges C, Ye L. Fusion Bonding of Polymer Composites. London: Springer, 2002.

[8] Yuan Q, Hou M, Mai YW, Ye L, Resistance welding of carbon fiber reinforced polyetherimide composite. Journal of Thermoplastic Composite Materials 2001; 14: 2-19.

[9] Hou M, Yang M, Beehag A, Mai YW, Ye L. Resistance welding of carbon fibre reinforced thermoplastic composite using alternative heating element. Composite Structures 1999; 47: 667-672.

[10] Dubé M, Hubert P, Gallet JNAH, Stavrov D, Bersee HEN, Yousefpour A. Metal mesh heating element size effect in resistance welding of thermoplastic composites. Journal of Composite Materials 2011; 46(8): 911-919.

[11] Shi H, Villegas IF, and H.E.N. Bersee HEN. Strength and failure modes in resistance welded thermoplastic composite joints: Effect of fibre-matrix adhesion and fibre orientation. Composites: Part A 2013; 55: 1-10.

[12] Ageorges C, Yen L, Hou M. Experimental investigation of the resistance welding of thermoplastic-matrix composites. Part II: Optimum processing window and mechanical performance. Composites Science and Technology 2000; 60: 1191-1202.

[13] Ageorges C, Ye L, Mai YW, Hou M. Characteristics of resistance welding of lap-shear coupons. Part III. Crystallinity. Composites Part A 1998; 29A*:* 921-932*.*

[14] Hou M, Ye L, Mai YW, An experimental study of resistance welding of carbon fibre reinforced polyetherimide (CF fabric/PEI) composite material. Applied Composite Materials 1999; 6: 35-49.

[15] Composite Materials Handbook. USA: Department of Defense Handbook. Vol. 3, 2002.

[16] Zhang Y, Vassilopoulos AP, Keller T. Effects of low and high temperatures on tensile behaviour of adhesively-bonded GFRP joints, Composite Structures 2010; 92: 1631-1639.

[17] Ashcroft IA, Hughes DJ, Shaw SJ, Abdel Wahab M, Crocombe A. Effect of temperature on the quasi-static strength and fatigue resistance of bonded composite double lap joints, J. Adhesion 2001; 75: 61-88.

[18] Adams RD, Coppendale J, Mallick V, Al-Hamdan H. The effect of temperature on the strength of adhesive joints. International Journal of Adhesion and Adhesives 1992; 12(3): 185-190.

[19] da Silva LFM, R.D. Adams RD. Effect of temperature on the mechanical and bonding properties of a carbon-reinforced bismaleimide. Journal of Materials: Design and Applications 2008; 222(1): 45-52.

[20] da Silva LFM, Adams RD. Joint strength predictions for adhesive joints to be used for a wide temperature range. International Journal of Adhesion and Adhesives 2007; 27: 362-379.

[21] Ahmed TJ. Hybrid composite structures: Multifunctionality through metal fibres*.* Delft: Delft University of Technology, 2009.

[22] Shi H. Resistance welding of thermoplastic composites. Process and performance. Delft: Delft University of Technology, 2014.

[23] ASTM Standard D 3518/D 3518M – 94, 2001, “Standard Test Method for In-Plane Shear Response of Polymer Composite Materials by Tensile Test of a ±45° Laminate”, ASTM International, West Conshohocken, PA.

[24] Madhukar MS, Drzal LT. Fiber-matrix adhesion and its effect on composite mechanical properties: I. Inplane and interlaminar shear behavior of graphite/epoxy composites. Journal of Composite Materials 1991; 25: 932-956.

[25] Wisnom MR. The effect of fibre rotation in ±45° tension tests on measured shear properties. Composites 1995; 26: 25-32.

[26] ASTM Standard D 1002 – 05, 2005, “Standard Test Method for Apparent Shear Strength of Single-Lap-Joint Adhesively Bonded Metal Specimens by Tension Loading (Metal-to-Metal), ASTM International, West Conshohocken, PA.

[27] Davis JR. Stainless Steels, ASM Specialty Handbook. Ohio: ASM International, 1994.

[28] Daniel IM, Ishai O. Engineering Mechanics of Composite Materials. New York: Oxford University Press, 2nd edition, 2006.

[29] Gleich DM, Van Tooren MJL, Beukers A. Analysis and evaluation of bondline thickness effects on failure load in adhesively bonded structures. Journal of Adhesion Science and Technology 2001; 15: 1091-1101.

[30] Guess TR, Allred RE, Gerstle FP. Comparison of lap shear test specimens. Journal of Testing and Evaluation 1977; 5: 84-93.

[31] Thomason JL, Yang L. Temperature dependence of the interfacial shear strength in glass-fibre polypropylene composites. Composites Science and Technology 2011; 71: 1600-1605.

[32] Carnevale P. Fibre-matrix interfaces in thermoplastic composites. Delft: Delft University of Technology, 2014.

[33] Rao V, Drzal LT. The temperature dependence of interfacial shear strength for various polymeric matrices reinforced with carbon fibers. Journal of Adhesion 1992; 37: 88-95.

[34] Lee S, Munro M, Scott RF. Evaluation of three in-plane shear test methods for advanced composite materials. Composites 1990; 21 (6): 495-502, 1990.

[35] Deng S, Ye L. Influence of fiber-matrix adhesion on mechanical properties of graphite/epoxy composites: II. Interlaminar fracture and inplane shear behaviour. Journal of Reinforced Plastics and Composites 1999; 18: 1041-1057.

[36] Da Silva LFM, Öchsner A. Modeling of Adhesively Bonded Joints. Heidelberg: Springer, 2008

[37] Zhao T, Palardy G, Villegas IF, Rans C, Martinez M, Benedictus R. Mechanical behaviour of thermoplastic composites spot-welded and mechanically fastened joints: a preliminary comparison. Composites Part B: Engineering 2017; 112: 224-234.

[38] Adams RD Adhesive Bonding: Science, Technology and Application. Boca Raton FL: Woodhead Publishing Limited and CRC Press LLC, 2005.

[39] Tsai MY, Oplinger DW, Morton J. Improved theoretical solutions for adhesive lap joints. Int. J. Solids Structures 1998; 35 (12): 1163-1185.